Y-2087

COMPOSITE FLYWHEEL DEVELOPMENT

(January 1 - March 31, 1977)

R. L. Huddleston
J. J. Kelly
C. E. Knight

September 1977

UNION CARBIDE

OAK RIDGE Y-12 PLANT
OAK RIDGE, TENNESSEE

prepared for the **U.S. ENERGY RESEARCH AND DEVELOPMENT ADMINISTRATION**
under **U.S. GOVERNMENT** *Contract W-7405 eng 26*

DISCLAIMER

Reference to a company or product name does not imply approval or recommendation of the product by Union Carbide Corporation or the U.S. Energy Research and Development Administration to the exclusion of others that may meet specifications.

Printed in the United States of America. Available from
National Technical Information Service
U.S. Department of Commerce
5285 Port Royal Road, Springfield, Virginia 22161
Price: Printed Copy ~~$3.50~~ 4.50 ; Microfiche $3.00

Y-2087

Date of Issue: September 19, 1977
Distribution Category: UC-94b

COMPOSITE FLYWHEEL DEVELOPMENT

(January 1 - March 31, 1977)

R. L. Huddleston
J. J. Kelly
C. E. Knight

Fabrication Systems Department
Y-12 Development Division

Oak Ridge Y-12 Plant
P. O. Box Y, Oak Ridge, Tennessee 37830

Prepared for the US Energy Research
and Development Administration
Under US Government Contract W-7405-eng-26

HIGHLIGHTS

A design concept was generated for the instrumented containment assembly.

Analytical results indicate that both the "dead-weight-loaded bandwrap" flywheel and the "prestressed-rim bandwrap" flywheel should significantly outperform Union Carbide Corporation-Nuclear Division's FY 1976/76T "bandwrap composite" flywheel.

Analytical results to date indicate that the use of a hybrid rim with two or more materials of different elastic moduli, such as Kevlar-29/epoxy overwrapped with Kevlar-49/epoxy, should improve the flywheel performance.

Additional transverse tensile characterization of Kevlar-49/epoxy, using three different room-temperature-curing epoxy resin formulations, resulted in no significant improvement over the approximately 1-ksi strength level previously attained in the FY 1976/76T flywheel.

CONTENTS

Previous reports in the series on Flywheel Development have Document Numbers Y-2072, Y-2080, and Y-2081.

COMPOSITE FLYWHEEL DEVELOPMENT

INTRODUCTION

This report summarizes Union Carbide Corporation-Nuclear Division's (UCC-ND's) Composite Flywheel Program status and results for the second quarter of FY 1977 (January 1 - March 31, 1977). This work was conducted for and funded by the Advanced Physical Methods Branch, Division of Energy Storage Systems, Office of Conservation, ERDA, Washington, DC.

As a part of its energy conservation program, ERDA is developing a heat-engine/flywheel hybrid vehicle. This goal will be accomplished by incorporating a high-speed flywheel energy storage system into a heat-engine vehicle. The flywheel system will be designed for peak energy storage and retrieval to promote more efficient engine operation and, also, to provide a system for regenerative braking.

PRIOR WORK

This program was initiated in May 1976. The first program phase, which was carried out during FY 1976/76T, was devoted to utilizing state-of-the-art UCC-ND technology to design, fabricate, and successfully spin test a nominal 0.5-kWh, 24.5-lb, 20-in-D, vehicular Kevlar/epoxy flywheel. The average energy density attained for the combined flywheel and hub was 10.1 watt hours per pound (Wh/lb).[1] During the first quarter of FY 1977, design concepts were generated for improving the FY 1976/76T flywheel performance, and an analytical evaluation of these concepts by finite-element analysis techniques was begun. A rotational catenary shape for the outer rim of the "bandwrap" flywheel was analytically generated. Finite-element analysis of the "bandwrap" flywheel with dead-weight loading indicated that a significant performance improvement over the FY 1976/76T flywheel is possible. Consequently, analytical and experimental investigations of the prestressed rim "bandwrap" flywheel design were initiated.[2]

FY 1977 PROGRAM OBJECTIVES

The overall objective of UCC-ND's program is to develop state-of-the-art, high-speed, composite flywheel and containment systems. The FY 1977 program encompasses the following technical objectives:

1. Design and fabricate an adequate, but not necessarily optimum, vehicular-sized containment housing and a special load-cell-instrumented mounting. The assembly will be designed for installation into a suitable spin test stand.

2. Design and fabricate an improved prototype composite flywheel which will be available for evaluation and burst testing in the instrumented containment package. Efforts will be keyed on developments which increase the energy density of the 0.5-kWh flywheel and hub assembly to a level above the 10.1 Wh/lb achieved in FY 1976T.

The containment package and composite flywheel will be available for test and evaluation by the end of this fiscal year. Subsequent burst testing of the composite flywheel and additional similar flywheels in the instrumented containment-mount assembly can provide a minimum amount of necessary data on transient loading and containment damage for design and development of a safe vehicular flywheel-containment system. Test and evaluation of the flywheel-containment-mount package is not covered by the current program objectives and funding level.

DEVELOPMENT PLANS

An updated schedule of tasks directed toward the design and fabrication of the FY 1977 flywheel and containment-mount assembly is summarized in Figure 1. A simplified schematic of the assembly mounted in a spin-test chamber is depicted in Figure 2.

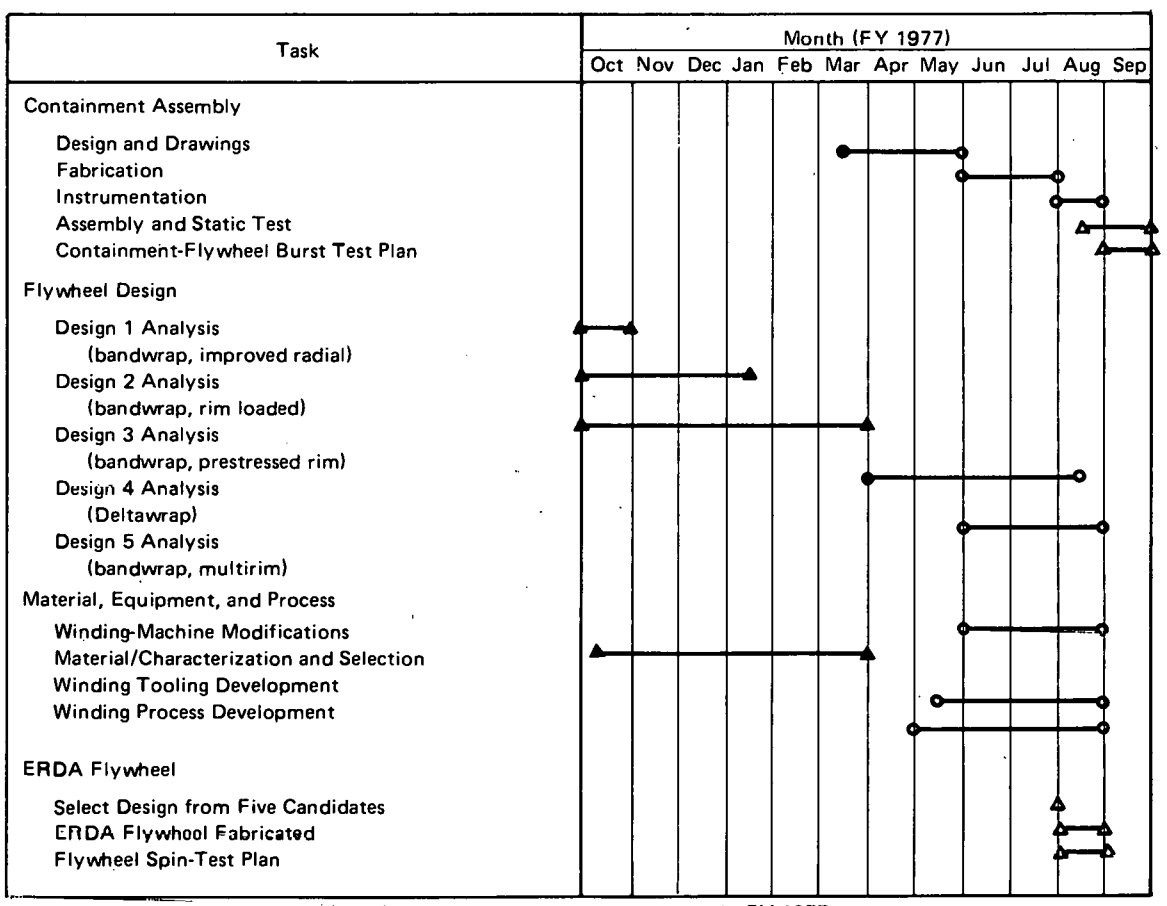

*Revised FY 1977 189 proposal issued reflecting no UCC-ND spin testing in FY 1077.

△ Target Dates
○ Modified Target Dates
●▲ Target Dates Achieved

Figure 1. MODIFIED DEVELOPMENT PLAN THAT LEADS TO THE FABRICATION OF AN IMPROVED COMPOSITE FLYWHEEL AND AN INSTRUMENTED CONTAINMENT-MOUNT ASSEMBLY. (Work to be completed by September 30, 1977)

CONTAINMENT ASSEMBLY DEVELOPMENT

Design of the containment assembly is still in the preliminary stage, as noted in the revised development plan (Figure 1). A conceptual drawing of the assembly is given in Figure 3. Instead of the interrupted bolted flange on the upper portion, the flange will likely be a continuous one that is sandwiched between two flanges supported from the outer ring (ie, ultimately from the vehicle) with discrete holes for rigid bolting in some tests. This arrangement permits evaluation of containment and mount loadings for both relatively hard-mounted and soft-mounted containment. It also permits removal of the lower torque tube, allowing the containment housing to rotate

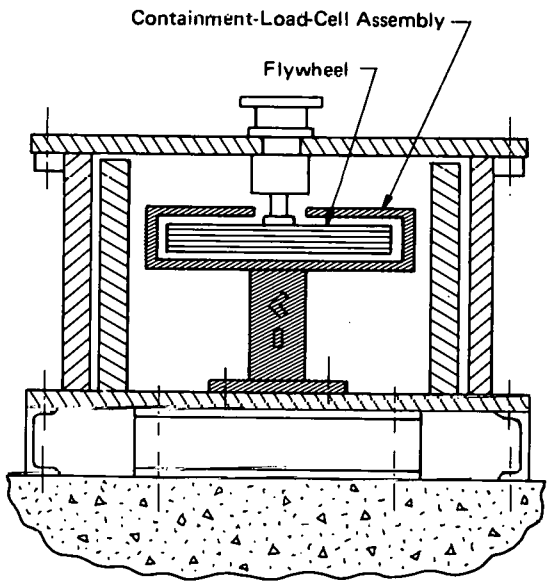

Figure 2. FLYWHEEL CONTAINMENT PACKAGE. (FY 1977 Design for Installation into a Suitable Spin Test Stand, as Shown)

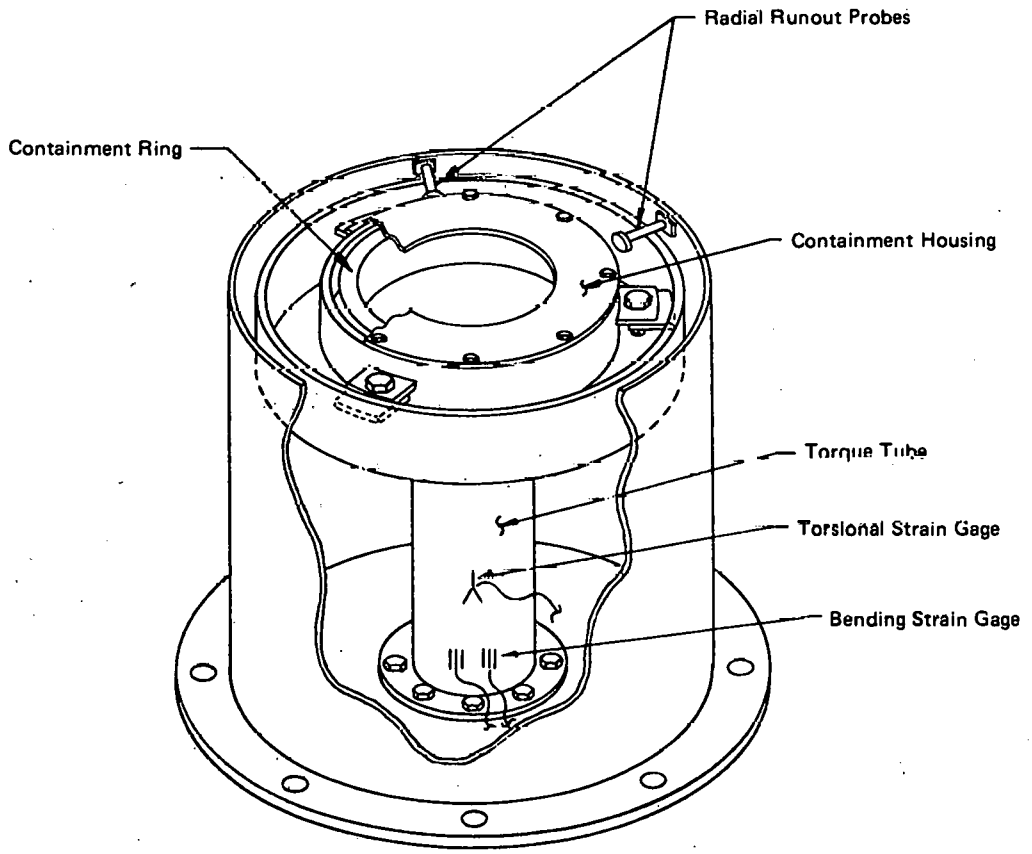

Figure 3. INSTRUMENTED CONTAINMENT HOUSING CONCEPT.

during flywheel failures for evaluation of braking materials inserted into the sandwiched flange.

Low-shear bolts or pins could also be evaluated with the housing rotating and being friction braked to a stop after a catastrophic flywheel failure. This concept also permits the placing of a second containment ring inside the containment housing for containment-material evaluations.

A minimum-weight, total vehicle containment package can be visualized that consists of an outer metallic vacuum housing with an inner light-weight composite containment ring supported in the vehicle by a friction-brake-type continuous flange. Detailed design of the instrumented containment assembly for ERDA will be done during the next quarter.

As noted in the development plan, the schedule of activities leading to fabrication and static testing of the hardware by September 30, 1977 was adjusted during this quarter to provide more efficient meshing of this effort with other on-going activities. Rescheduling of these tasks will not affect the final completion date.

FLYWHEEL DEVELOPMENT ACTIVITIES

Rotor development during this quarter has concentrated on further design alternatives for the "bandwrap" flywheel, and design and analysis of the Deltawrap flywheel was started. Also, the transverse tensile strength of several other composite systems was determined. A prestressed rim and a mixed-material rim of Kevlar-29 and Kevlar-49 were the bandwrap design alternatives that were evaluated.

Two small-scale test rims were wound for establishing the potential for prestressing rims. In each test, the rim inner layers failed in compression when the winding was completed. Results from these tests indicate that a near-optimum prestress can be achieved. Calculations for a mixed-material rim show that a rim of nearly a 0.78 overall radius ratio would have radial tensile stresses approximately 25% of those in the single-material rim.

A finite-element model is in preparation for the Deltawrap flywheel, and the design concept is established. Also, an overwrap thickness profile and angle-ply fiber orientation computer program were developed. In addition, transformed material properties were the output from the program.

Transverse Strength Characterization

One of the critical factors in the application of thick-rim flywheels is the composite strength or failure strain transverse to the fiber. The first flywheel test in this program failed in transverse or radial tension in the Kevlar/epoxy rim. The failure occurred at a calculated stress level of approximately 1 ksi. Transverse-tension flexure tests reported in the FY 1976/76T Composite Flywheel Development Report[1] on the material system used in the tested flywheel confirmed this failure stress level.

The specimens used in the test results reported previously were machined from wound cylinders; and, due to the difficulty in machining Kevlar/epoxy composites, the specimens were not of the highest quality. This problem may have contributed to the high data variability and degraded the tensile-strength values. New specimens were produced by fabricating rings with an as-wound cross section of a 0.500-in by 0.500-in nominal size. The rings were cut into three segments for flexure tests. Two of the Kevlar/epoxy material systems reported previously[1] were tested again with new rings.

The tests conducted this quarter are summarized in Table 1. The first material-system results are 26% lower than previously reported, but the variability has improved by 60%. The

Table 1

TRANSVERSE TENSILE STRENGTH OF SELECTED COMPOSITES

Material System	Quantity (vol %) Fiber	Resin	Void	Tensile Strength (psi)	Maximum Hoop Compressive Stress (ksi)	Modulus of Elasticity (msi)
Kevlar-49/ (DER332/T403)	74.5	22.9	2.6	870 (CV = 18.2%)(2)	23	0.89
Kevlar-49/ (XD7818/D230/A398)	76.0	22.8	1.2	1000 (CV = 12.8%)	26	0.94
Kevlar-49/ (DER332/T403/A398)	72.9	24.6	2.5	960 (CV = 10.9%)	25	0.82
S-glass/ (DER332/T403)	74.0	22.2	3.8	2920 (CV = 1.3%)	75	2.95
S-glass/ (ERL2258/MPDA)	74.9	22.1	3.0	3380 (CV = 10.0%)	89	3.18
3M SP308 Kevlar-49 prepreg				1975 (CV = 24.6%)		0.72

(1) DER332 and XD7818 are products of Dow Chemical; T403, D230, and A398 are products of Jefferson Chemical; ERL2258 is a product of Union Carbide; MPDA is metaphenylenediamine, a standard chemical product; 3M SP308 is a product of 3M.

(2) Coefficient of variation, CV = (standard deviation/mean) x 100 percent.

second material-system results are improved over those previously reported by 72%, and the variability is improved by 250%. An additional Kevlar/epoxy system and two S-glass/epoxy system flexure tests are also reported. The last material system is the 3M Company SP-308 Kevlar/epoxy prepreg. These specimens were straight-sided transverse tensile coupons. This material has a literature-reported strength of 4 ksi, but that was not achieved in these tests. Scanning electron microscope (SEM) views of the fracture surface in this material are presented in Figure 4. In comparison with the SEM views of the composite fracture surface shown last quarter,[2] there appears to be some improvement in resin wetting and bonding to the fiber.

Experience with low-void-content (< 0.5%) S-glass/epoxy composites reveals that the results reported in Table 1 are low by a factor of two or three. If special resin-impregation

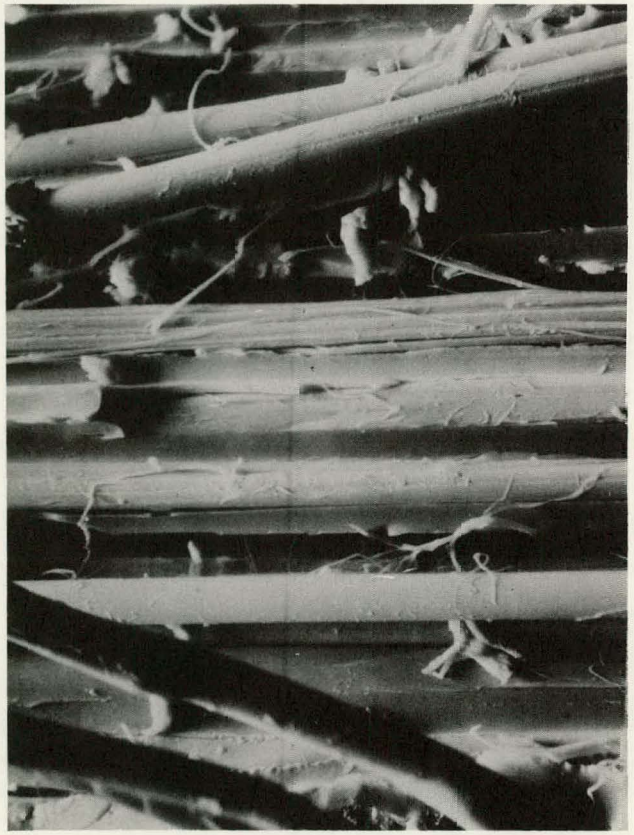

SM-77-0046-10

(a) At 500X.

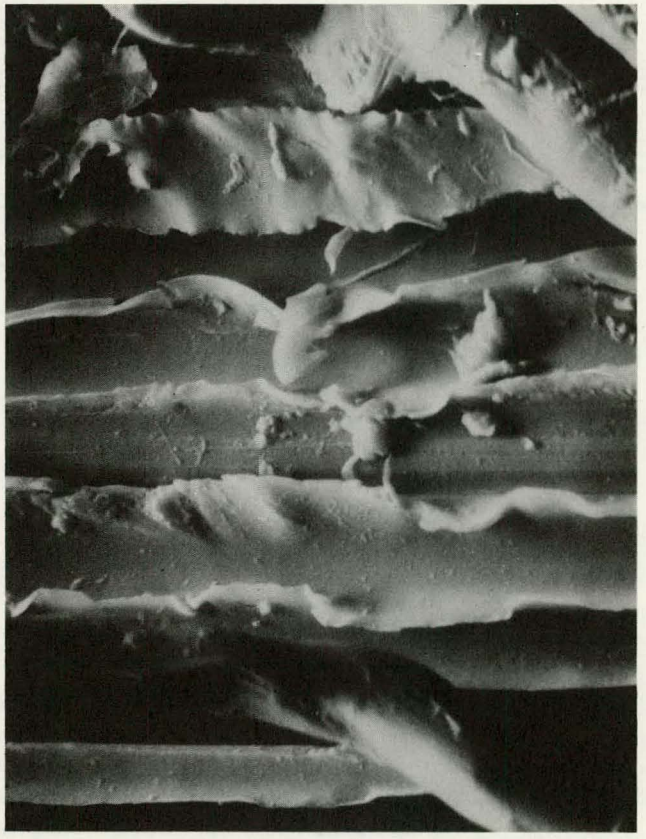

SM-77-0046-9

(b) At 1000X.

Figure 4. FRACTURE SURFACE OF THE 3M SP308-KEVLAR/EPOXY PREPREG TRANSVERSE TENSILE SPECIMEN.

techniques are employed to lower the void contents of these composites, certainly the S-glass/epoxy data would improve; and, possibly, the Kevlar/epoxy data would also improve.

The maximum hoop compressive flexure stress is monitored to be sure that the composite fails in transverse tension. The stress/strain response was linear to failure in all these tests, so the failure strains may be easily calculated.

Prestressed Rim Evaluation

The theory for producing a prestressed rim by means of winding tension control in wound and cured layers was presented last quarter.[2] The built-in stress distributions for a given tension schedule are calculated by use of the equations. A calculated prestress condition was presented for a prescribed tension schedule. A test ring has been wound for evaluation of that schedule.

The mandrel was a steel cylinder (6" OD x 0.040" T). The mandrel was strain gaged on the inside, and the strains were monitored as the layers were wound. Ten layers (each, 0.100 inch thick) were wound. A layer was wound and allowed to cure at room temperature before winding the next layer. Strains were monitored when the layer was completed and still wet and then when it was cured. There was only a slight relaxation during layer curing. The strain increment when a layer is applied and the properties of the composite-plus-mandrel cylinder to which the layer is applied are used to calculate the actual retained tensile stress in the applied layer. The calculation is performed for each layer and the results superimposed to find the resultant prestress distributions.

Table 2 summarizes the calculated-versus-realized parameters in the first test ring. The actual retained tensile stress in the layers deviated significantly from the desired levels. The reason for this deviation is not clear; but, it could be due to a variation in the winding tension,

Table 2

PRESTRESS RESULTS IN TEST RIM 1
(380 Denier Kevlar-49 Yarn)

Applied Winding Tension (g)	Retained Layer Stress (ksi)		Layer Inside Radius (in)	Radial Stress (ksi)		Hoop Stress (ksi)	
	Theoretical	Experimental		Theoretical	Experimental	Theoretical	Experimental
275	0	2	3.0	0	0	-66.6	-69.0
600	11	11	3.1	-2.12	-2.23	-54.1	-53.7
925	22	20	3.2	-3.66	-3.83	-38.2	-37.0
1250	33	33	3.3	-4.61	-4.84	-21.2	-15.9
1600	44	41	3.4	-5.00	-5.17	- 3.5	1.2
1925	55	72	3.5	-4.84	4.98	15.0	46.8
1925	55	50	3.6	4.17	-3.54	23.2	32.6
1925	55	50	3.7	-3.33	-2.57	30.7	40.3
1925	55	27	3.8	-2.34	-1.43	37.7	20.6
1925	55	36	3.9	-1.23	-0.89	44.6	34.6
			at r = 4.0	0	0	51.3	34.6

variation in the resin viscosity, and/or inaccurate strain-gage readings. The control seems to be much more erratic after the mandrel has yielded, which occurred as Layer 5 was applied. This result would seem to indicate inaccurate strain-gage readings due to plastic mandrel strain.

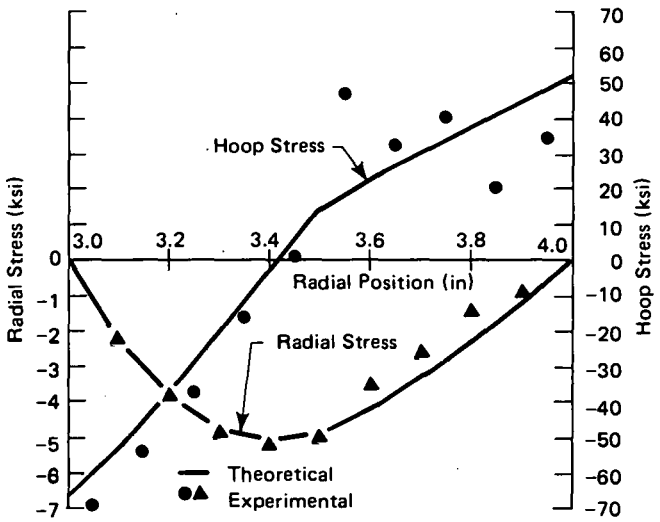

Figure 5. THEORETICAL VERSUS EXPERIMENTAL RESIDUAL STRESS DISTRIBUTION IN TEST RIM 1.

The theoretical-versus-experimental prestress distributions are shown by the graph of Figure 5. The deviations previously mentioned appear in these distributions. If the strain-gage readings are not reliable, then the actual distributions may be closer to the theoretical. The inner layers of the ring experienced a hoop-compressive microbuckling-type failure when the steel mandrel was removed. This action occurred at a calculated stress level between 65 and 69 ksi. Measurement of the ring inside diameter compared well with the total strain readings, confirming this stress level. Failure of the inner layers prevented a residual stress analysis by incremental material-removal techniques.

By manipulation of parameters in the equations predicting the prestress, it is determined that a lower-stiffness mandrel produces the highest prestress level for a given maximum winding tension. Additionally, the best tension schedule to balance the radial-stress distribution in the 0.75-radius-ratio rim is a linear variation from zero tension in the inner layer to maximum tension in the outer layer.

A second winding-tension schedule was developed for test and evaluation. Plexiglas was selected for the mandrel material to give a low stiffness as well as provide a linear stress/strain response through the strain range imposed during the test winding. The theoretical schedule limits the inner-layer compressive stress to 50 ksi and produces a maximum radial compressive stress of 4.1 ksi.

Table 3 summarizes the Schedule 2 parameters and gives the results of the test winding. The retained tensile stress in the wound layers, on the average, exceeded the desired levels by 19%. The resultant stress distributions are compared with the theoretical distributions in Figure 6. The agreement is much better on this test ring, but the excess retained tension caused this ring to fail also by an inner-layer-microbuckling compressive failure. The failure occurred while the final layer was curing, and the inner layer stress was 65 ksi compression.

These two test rings demonstrate the capability to achieve prestress levels that can effectively eliminate radial tensile stress on the composite rim. The control as yet is not satisfactory, but should improve with additional development.

Table 3

PRESTRESS RESULTS IN TEST RIM 2
(380 Denier Kevlar-49 Yarn)

Applied Winding Tension (g)	Retained Layer Stress (ksi)		Layer Inside Radius (in)	Radial Stress (ksi)		Hoop Stress (ksi)	
	Theoretical	Experimental		Theoretical	Experimental	Theoretical	Experimental
250	0	0.7	3.0	0	0	-50.0	-66.2
475	6.5	8.3	3.1	-1.60	-2.14	-42.4	-50.2
650	13.0	14.4	3.2	-2.80	-3.64	-31.6	-37.5
850	19.4	21.4	3.3	-3.59	-4.67	-20.6	-24.3
1040	25.9	30.0	3.4	-4.02	-5.25	- 9.5	- 9.5
1250	32.4	34.8	3.5	-4.11	-5.37	1.7	1.1
1425	38.9	44.0	3.6	-3.87	-5.19	13.2	16.8
1625	45.4	59.5	3.7	-3.34	-4.60	25.2	40.6
1825	51.9	65.4	3.8	-2.51	-3.41	37.6	55.1
2000	58.4	75.0	3.9	-1.40	-1.91	50.7	74.3
			at r = 4.0	0	0	58.1	74.3

Hybrid Kevlar Rim

One of the concepts for controlling radial stress is the use of graded elastic properties in the rim. If the hoop modulus, in particular, could be continuously variable with radial position from a low value at the inside radius to a high value at the outside, the radial stress could be theoretically eliminated. In the practical sense, however, this material (with a continuously variable modulus) does not exist.

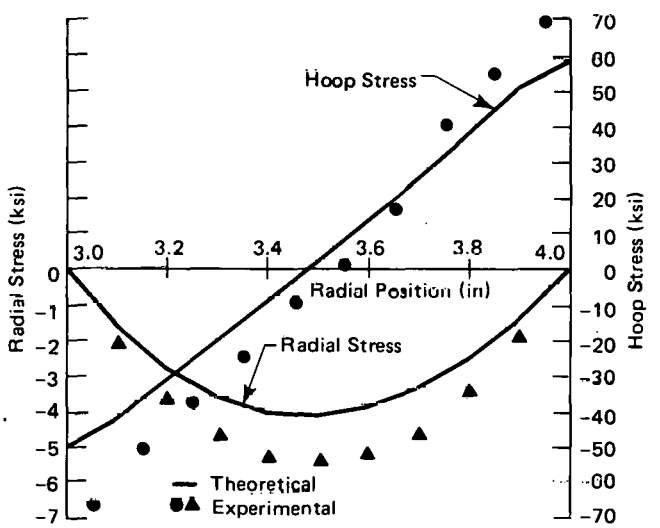

Figure 6. THEORETICAL VERSUS EXPERIMENTAL RESIDUAL STRESS DISTRIBUTION IN TEST RIM 2.

There are a number of high-performance composite materials with different values of longitudinal elastic modulus such as fiberglass, graphite, boron, and two types of Kevlar. The two types of Kevlar available have a modulus ratio that looks particularly beneficial for combination in a thick rim. The fiber modulus of Kevlar-49 is reported to be 19 msi and of Kevlar-29 is 9 msi.[3] The composite hoop moduli reported were 11.0 and 7.25 msi, respectively, at 60 vol % fiber (the value on Kevlar-29 does not agree with the rule-of-mixtures calculation). The flywheel rims have had a fiber volume fraction of approximately 70%. Ratioing the given moduli for a 70% fiber composite gives moduli of 12.8 and 8.5 msi, respectively.

Assume the rim to be made of Kevlar-29 in the inner half and Kevlar-49 in the outer half, the peak radial tensile stress occurs very near the rim midpoint. Using the previously defined elastic properties, calculator solutions for the orthotropic rotating ring were obtained for

given radius-ratio rims. By trial and error, the overall rim-radius ratio was found which matched displacements at the Kevlar-29 and Kevlar-49 interface. This radius ratio is 0.782 (r_i/r_o). The interface, then, has a zero radial stress. The maximum radial tensile stress is 1.3 ksi in the outer half at a speed where the hoop stress is 250 ksi. The corresponding rim of all Kevlar-49 has a radial stress of 5.9 ksi at that speed. If the overall radius ratio on the hybrid rim is lower than 0.782, then interface tension exists and adds to the maximum radial tensile stress; if the overall radius ratio is higher (thinner rim), then interface compression exists and decreases the radial tensile stress.

This Kevlar combination looks like it would make a potentially effective hybrid rim. It only needs a more detailed design study to select the proper combination. Obviously, the individual rim portions could be prestressed, and an interference condition could be built in at the Kevlar-29/Kevlar-49 interface.

Deltawrap Flywheel Design

The Deltawrap flywheel design concept was presented in a previous quarterly report,[4] where a number of concepts were catalogued. The essence of this design is the use of a set of parallel filament bands for an overwrap around a circumferentially wound rim. The parallel filament bands provide a continuous coverage and minimize hub-thickness buildup of the overwrap winding. The overwrap is designed to provide external pressure on the rim and, thus, allow a higher operating speed than for the free rim. The overwrap also provides a stiff coupling from the rim to shaft to raise the critical vibration speeds.

The overwrap is a variable-thickness, variable-fiber-orientation, structural component. This combination complicates the analysis and requires preparation of a computer program to calculate the thickness profile and fiber-orientation angle as a function of the radial position. The thickness profile is then modeled by the finite-element mesh for analysis. The varying fiber orientation causes the material properties to vary and must be accounted for in the model.

Calculation of thickness and fiber angle is based on the geometrical considerations illustrated in Figure 7. At any given radial coordinate, r, the thickness calculation is based

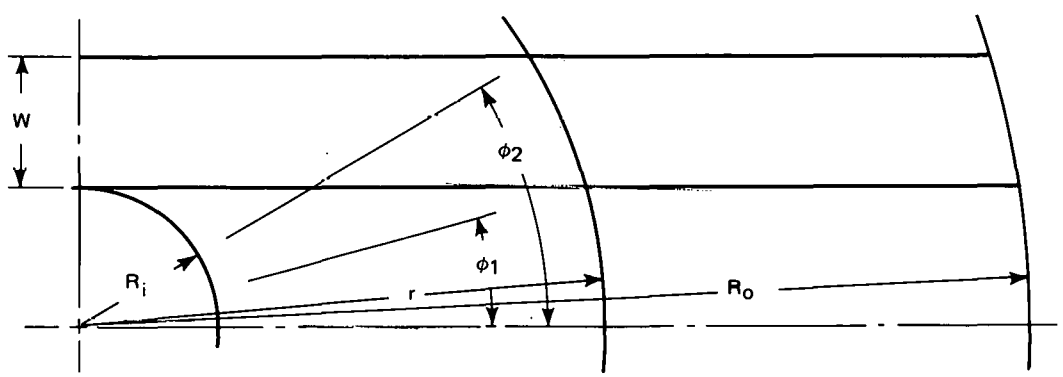

Figure 7. GEOMETRICAL RELATIONSHIP FOR CALCULATING THE OVERWRAP-THICKNESS PROFILE AND FIBER ANGLE.

on the arc coverage of a band on the circle of radius, r, the number of bands, and the band thickness. The thickness is calculated by the equation:

$$t = r(\phi_2 - \phi_1)\frac{2N}{\pi r} t_b$$

where:

t represents the thickness buildup,

ϕ_2 and ϕ_1 the angles shown (Figure 7),

N the number of bands in the set, and

t_b the band thickness.

Along the inner band edge, the angle is:

$$\phi_1 = \sin^{-1}\frac{R_i}{r} ;$$

along the outer edge, the angle is:

$$\phi_2 = \frac{\pi}{2} \text{ , for } R_i \leqslant r \leqslant R_i + W, \text{ and}$$

$$\phi_2 = \sin^{-1}\frac{R_i + W}{r} \text{ , for } R_i + W \leqslant r \leqslant R_o ,$$

where:

R_i represents the inner radius of the band set,

W the band width, and

R_o the outer radius of the band set.

The fiber orientation angle with respect to the radial direction varies between ϕ_1 and ϕ_2 at the radial position, r. The average of ϕ_1 and ϕ_2 is specified as the fiber angle at radius r. The thickness profile and fiber angle are plotted in Figure 8 for the case of R_i = 0.750 inch, R_o = 10.0 inches, W = 0.750 inch, t_b = 0.003 inch, and N = 40 bands.

The fiber-angle variation with the radial coordinate, of course, causes the material properties, with respect to the radial-hoop coordinates, to vary. The fiber-angle variation between ϕ_1 and ϕ_2 at a given radial coordinate also causes the properties to vary. There are a number of approaches to find the material-stiffness matrix which will represent the oriented material at the given radial position. The composite is modeled as a symmetric angle-ply laminate. The first option is between bonded plies and unbonded (shear-failure) plies. On initial loading, the plies are bonded; and, prior experience with angle-ply wound structures, indicates that they remain bonded up to the ultimate laminate strength.

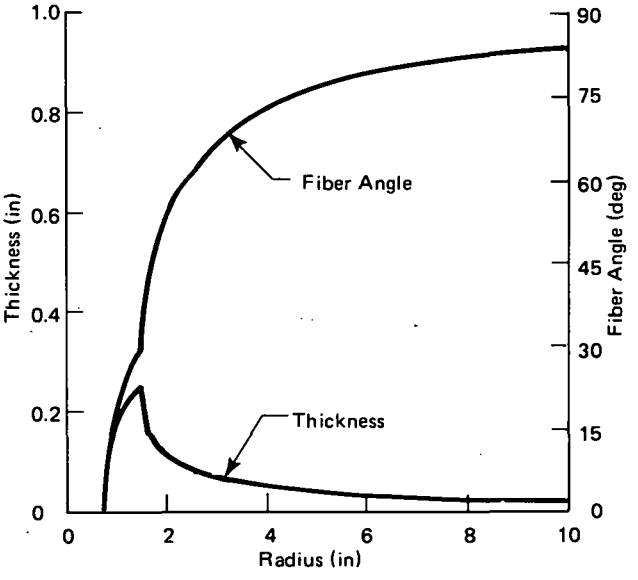

Figure 8. THICKNESS AND FILM-ANGLE PROFILE OF THE OVERWRAP ON THE DELTAWRAP FLYWHEEL.

The next option is whether to calculate the properties for the average fiber angle at a given radial position or calculate properties for the range of fiber angles at that position and average the material-stiffness matrices. Since the material-stiffness matrix transforms with the angle as a fourth-rank tensor, the resulting stiffness matrix for the two approaches will not be the same. The latter approach is more involved, but should be more representative of the average material at a given position and is the approach used. This approach demands that the calculations be performed in the thickness and fiber-angle program rather than in the finite-element code. The average material properties are derived from this stiffness matrix and output with the thickness and average fiber angle for each specified radial coordinate. The computer program listing and the output corresponding to that in Figure 8 are given in the Appendix. This output is then used to prepare the input for the finite-element program.

The selected radii-to-output data from the thickness calculation program should correspond to the finite-element mesh used to analyze the structure. Since the material properties vary with the radial position, a different material type will have to be assigned at each radial position unless the property values are reasonably close for two or more positions.

A finite-element model is in preparation to analyze a proposed design. The finite-element code will have to be modified to accept a greater number of material types, and calculational steps must be added to compute stress and strain components with respect to a principal fiber coordinate system.

FUTURE WORK

Tasks to be accomplished during the next quarter include designing and initiating fabrication of the instrumented containment package and additional flywheel design and analysis work.

Additional development of prestressed rims is also planned for next quarter. Better control and establishment of prestress level limits for use in operating flywheel rims are the primary goals. A finite-element stress analysis will be performed on the Deltawrap Flywheel design. Fabrication methods for the Deltawrap design will be developed. Additional design alternatives for the "bandwrap" flywheel design will be analytically evaluated.

REFERENCES

1. Huddleston, R. L., Kelly, J. J., and Knight, C. E., Jr; ***Composite Flywheel Development Completion Report (May 1 - September 30, 1976)***, Y-2080; Union Carbide Corporation-Nuclear Division, Oak Ridge Y-12 Plant, Oak Ridge, Tennessee; May 11, 1977.

2. Huddleston, R. L., Kelly, J. J., and Knight, C. E., Jr; ***Composite Flywheel Development (October 1 - December 31, 1976)***, Y-2081; Union Carbide Corporation-Nuclear Division, Oak Ridge Y-12 Plant, Oak Ridge, Tennessee; May 11, 1977.

3. Riewald, P. G., and Zweben, C.; ***Kevlar-49 Hybrid Composites for Commercial and Aerospace Applications***; Paper Given at the 30th Annual SPI Technical Conference (1975).

4. Huddleston, R. L., Kelly, J. J., and Knight, C. E., Jr; ***Composite Flywheel Development (May 1 - June 30, 1976)***, Y-2072; Union Carbide Corporation-Nuclear Division, Oak Ridge Y-12 Plant, Oak Ridge, Tennessee; January 24, 1977.

APPENDIX

METHOD FOR TRANSFORMING COMPOSITE MATERIAL PROPERTIES AND CALCULATING THICKNESS BUILDUP IN THE OVERWRAP BANDS FOR THE DELTAWRAP FLYWHEEL

```
C. **********
C. THIS PROGRAM CALCULATES TRANSFORMED MATERIAL PROPERTIES OF
C. UNIDIRECTIONAL COMPOSITE MATERIAL ANGLE-PLY LAMINATES AND
C. THICKNESS BUILDUP AT SPECIFIED RADIAL COORDINATE POSITIONS
C. FOR THE OVERWRAP PORTION OF THE "DELTAWRAP" FLYWHEEL.
C. THE RADIUS, THICKNESS, AVERAGE FIBER ORIENTATION ANGLE, AND
C. THE AVERAGE TRANSFORMED MATERIAL PROPERTIES ARE OUTPUT.
C. **********
C. **********
C. THE FIRST LINE OF INPUT IS THE UNIDIRECTIONAL ELASTIC PROPERTIES
C. WITH THE 1 AXIS ALIGNED WITH THE FIBER DIRECTION.
C. RO IS THE HUB RADIUS OR INNER RADIUS OF COMPOSITE,
C. RM IS THE OUTSIDE RADIUS OF COMPOSITE,
C. W IS THE BAND WIDTH,
C. NB IS THE NUMBER OF BANDS IN THE SET,
C. TB IS THE BAND THICKNESS,
C. NEL IS THE TOTAL NUMBER OF ELEMENT ROWS IN THE MODEL,
C. REL(I) IS THE RADIAL COORDINATE CORRESPONDING TO NE(I),
C. NE(I) IS THE NUMBER OF ELEMENT ROWS TO COORDINATE REL(I),
C. NOTE:  REL(I) AND NE(I) ARE INPUT IN PAIRS UNTIL NE(I) EQUALS
C.        NEL (MAX OF 10 PAIRS) AND REL(1) = RO, NE(1) = 0.
C. **********
      REAL NU12,NU13,NU23,M,N,M2,N2,M4,N4,MN,NUNS,NUNT,NUST
      DIMENSION REL(10), NE(10), RTHK(100), THK(100)
      ACCEPT [E11,E22,E33,NU12,NU13,NU23,G12,G13,G23]
      ACCEPT [RO,RM,W,NB,TB,NEL]
      DO 1 I = 1,10
      ACCEPT [REL(I), NE(I)]
      IF(NE(1) .EQ. NEL) GO TO 2
    1 CONTINUE
    2 CONTINUE
      OPEN(3,OUTPUT,/TEMP/)
   10 V = 1./(1. - (NU12**2)*E22/E11 - (NU23**2)*E33/E22 - (NU13**2)

         *E33/E11 - 2.*NU12*NU23*NU13*E33/E11)
      C11 = (1. - (NU23**2)*E33/E22)*V*E11
      C22 = (1. - (NU13**2)*E33/E11)*V*E22
      C33 = (1. - (NU12**2)*E22/E11)*V*E33
      C12 = (NU12*E22/E11 + NU23*NU13*E33/E11)*V*E11
      C13 = (NU13*E33/E11 + NU12*NU23*E33/E11)*V*E11
      C23 = (NU23*E33/E22 + NU12*NU13*E33/E11)*V*E22
      C44 = G23
      C55 = G13
      C66 = G12
      RAD = 57.29577951
      PI = 3.141592654
      WRITE [1,101] E11,E22,E33,NU12,NU13,NU23,G12,G13,G23
      WRITE [1,104] RO,RM,W,NB,TB,NEL
      WRITE [1,103]
      II = 2
```

```
      DO 100 I = 1,NEL
      IF(I .GT. NE(II)) II = II+1
      R1 = REL(II-1)
      R2 = REL(II)
      DR = (R2-R1)/(NE(II) - NE(II-1))
      RANG = R1 + (I-NE(II-1))*DR - DR/2.
      RTHK(I) = R1 + (I-NE(II-1))*DR
      PHI2 = PI/2.
      IF(RTHK(I) .GT. RO+W) RTAN2 = SQRT(RTHK(I)**2 - (RO+W)**2)
      RTAN1 = SQRT(RTHK(I)**2 - RO**2)
      IF(RTHK(I) .GT. RO+W) PHI2 = ATAN((RO+W)/RTAN2)
      PHI1 = ATAN(RO/RTAN1)
      THK(I) = 2.*TB*NB*(PHI2 - PHI1)/PI
      PHI2 = 0.0
      DO 100 I = 1,NEL
      IF(I .GT. NE(II)) II = II+1
      R1 = REL(II-1)
      R2 = REL(II)
      DR = (R2-R1)/(NE(II) - NE(II-1))
      RANG = R1 + (I-NE(II-1))*DR - DR/2.
      RTHK(I) = R1 + (I-NE(II-1))*DR
      PHI2 = PI/2.
      IF(RTHK(I) .GT. RO+W) RTAN2 = SQRT(RTHK(I)**2 - (RO+W)**2)
      RTAN1 = SQRT(RTHK(I)**2 - RO**2)
      IF(RTHK(I) .GT. RO+W) PHI2 = ATAN((RO+W)/RTAN2)
      PHI1 = ATAN(RO/RTAN1)
      THK(I) = 2.*TB*NB*(PHI2 - PHI1)/PI
      PHI2 = 0.0
      IF(RANG .GT. RO+W) RTAN2 = SQRT(RANG**2 - (RO+W)**2)
      RTAN1 = SQRT(RANG**2 - RO**2)
      IF(RANG .GT. RO+W) PHI2 = ATAN(RTAN2/(RO+W))
      PHI1 = ATAN(RTAN1/RO)
      DPHI = (PHI1 - PHI2)/10.
      C11P = 0.0
      C22P = 0.0
      C12P = 0.0
      C33P = 0.0
      C13P = 0.0
      C23P = 0.0
      C55P = 0.0
      DO 50 J = 1,10
      BETA = PHI1 - J*DPHI + DPHI/2.
      M = SIN(BETA)
      N = COS(BETA)
      M2 = M**2
      N2 = N**2
      M4 = M**4
      N4 = N**4
      MN = M2*N2
   30 C11P =(M4*C11 + MN*(2.*C12 + 4.*C66) + N4*C22)/10. + C11P
      C22P =(N4*C11 + MN*(2.*C12 + 4.*C66) + M4*C22)/10. + C22P
      C12P =(MN*(C11 + C22 -4.*C66) + (M4+N4)*C12)/10. + C12P
      C33P = C33/10. + C33P
      C13P =(M2*C13 + N2*C23)/10. + C13P
      C23P =(N2*C13 + M2*C23)/10. + C23P
      C55P =(N2*C44 + M2*C55)/10. + C55P
   50 CONTINUE
      BETA = (PHI1 + PHI2)/2.
      X = C11P*C22P*C33P + 2.*C12P*C23P*C13P - C22P*C13P**2
```

```
      - C11P*C23P**2 - C33P*C12P**2
      S11P = (C22P*C33P - C23P**2)/X
      S22P = (C11P*C33P - C13P**2)/X
      S12P = (C13P*C23P - C12P*C33P)/X
      S13P = (C12P*C23P - C13P*C22P)/X
      S23P = (C12P*C13P - C23P*C11P)/X
      S55P = 1./C55P
   31 EN = E33
      ES = 1./S11P
      ET = 1./S22P
      NUNS = -EN*S13P
      NUNT = -EN*S23P
      NUST = -ES*S12P
      GNS = 1./S55P
      BETA = BETA*RAD
      WRITE(1,102) RTHK(I),THK(I),BETA,EN,ES,ET,NUNS,NUNT,NUST,GNS
      WRITE(3,(8F7.3)) BETA,EN,ES,ET,NUNS,NUNT,NUST,GNS
  100 CONTINUE
  101 FORMAT(////6HMODULI /6HE11 = F6.3/6HE22 = , F6.3/6HE33 = ,F6.3//

      16HPOISSON'S RATIOS /7HNU12 = F6.3/7HNU13 = F6.3/7HNU23 = F6.3//

      12HSHEAR MODULI /6HG12 = F6.3/6HG13 = F6.3/6HG23 = F6.3///)
  102 FORMAT (F7.3,F8.4,F6.1,3F7.2,4F7.3)
  103 FORMAT (//22X,42H-------MODULI-------  --POISSON'S RATIOS-  /

      7H RADIUS, 8H   THICK, 6H  BETA, 3X, 2HEN, 5X, 2HES, 5X,

      2HET, 4X, 4HNUNS, 3X, 4HNUNT, 3X, 4HNUST, 4X, 3HGNS //)
  104 FORMAT (4HRO =,F6.3/4HRM =,F6.3/3HW =,F6.3/4HNB =,I4/4HTB =,

             F6.4/5HNEL =,I4)
  200 CONTINUE
      CLOSE
      END
```

MODULI
E11 = 14.000
E22 = 0.800
E33 = 0.800

POISSON'S RATIOS
NU12 = 0.340
NU13 = 0.340
NU23 = 0.340

SHEAR MODULI
G12 = 0.300
G13 = 0.300
G23 = 0.300

RO = 0.750
RM =10.000
W = 0.750
NB = 126
TB =0.0030
NEL = 50

			-------MODULI-------			--POISSON'S RATIOS-			
RADIUS	THICK	BETA	EN	ES	ET	NUNS	NUNT	NUST	GNS
0.900	0.1409	12.3	0.80	0.82	11.56	0.313	0.005	0.077	0.300
1.050	0.1865	19.9	0.80	1.03	8.51	0.228	-0.003	0.159	0.300
1.200	0.2155	24.1	0.80	1.34	7.31	0.167	0.001	0.210	0.300
1.350	0.2363	27.0	0.80	1.66	6.75	0.131	0.007	0.244	0.300
1.500	0.2520	29.1	0.80	1.95	6.44	0.109	0.012	0.267	0.300
1.650	0.1610	39.7	0.80	2.24	3.60	0.068	0.022	0.494	0.300
1.800	0.1336	46.9	0.80	2.51	2.09	0.031	0.053	0.771	0.300
1.950	0.1162	51.6	0.80	2.88	1.48	0.006	0.095	1.007	0.300
2.100	0.1036	55.2	0.80	3.35	1.19	-0.010	0.137	1.207	0.300
2.250	0.0938	58.1	0.80	3.92	1.04	-0.019	0.174	1.368	0.300
2.600	0.0776	61.9	0.80	4.98	0.91	-0.023	0.222	1.550	0.300
2.950	0.0665	65.8	0.80	6.51	0.83	-0.020	0.265	1.648	0.300
3.300	0.0584	68.7	0.80	7.88	0.80	-0.015	0.289	1.623	0.300
3.650	0.0521	71.0	0.80	9.02	0.79	-0.010	0.304	1.536	0.300
4.000	0.0471	72.8	0.80	9.92	0.79	-0.005	0.313	1.426	0.300
4.350	0.0430	74.3	0.80	10.62	0.79	-0.001	0.319	1.313	0.300
4.700	0.0396	75.6	0.80	11.17	0.79	0.002	0.323	1.208	0.300
5.050	0.0367	76.6	0.80	11.61	0.79	0.004	0.326	1.114	0.300
5.400	0.0342	77.5	0.80	11.95	0.79	0.006	0.329	1.031	0.300
5.750	0.0320	78.3	0.80	12.23	0.79	0.008	0.330	0.959	0.300
6.100	0.0301	79.0	0.80	12.45	0.79	0.009	0.332	0.897	0.300
6.450	0.0284	79.7	0.80	12.64	0.79	0.010	0.333	0.842	0.300
6.800	0.0269	80.2	0.80	12.79	0.79	0.011	0.334	0.795	0.300
7.150	0.0256	80.7	0.80	12.92	0.79	0.012	0.334	0.754	0.300
7.500	0.0244	81.2	0.80	13.03	0.79	0.012	0.335	0.718	0.300
7.611	0.0240	81.4	0.80	13.10	0.79	0.013	0.335	0.697	0.300
7.722	0.0236	81.6	0.80	13.12	0.79	0.013	0.336	0.687	0.300
7.833	0.0233	81.7	0.80	13.15	0.79	0.013	0.336	0.678	0.300
7.944	0.0230	81.8	0.80	13.18	0.79	0.013	0.336	0.669	0.300
8.056	0.0226	81.9	0.80	13.20	0.79	0.014	0.336	0.660	0.300
8.167	0.0223	82.0	0.80	13.23	0.79	0.014	0.336	0.652	0.300

8.278	0.0220	82.1	0.80	13.25	0.79	0.014	0.336	0.644	0.300
8.389	0.0217	82.2	0.80	13.27	0.79	0.014	0.336	0.636	0.300
8.500	0.0214	82.3	0.80	13.29	0.79	0.014	0.336	0.629	0.300
8.611	0.0211	82.4	0.80	13.31	0.79	0.014	0.337	0.621	0.300
8.722	0.0209	82.5	0.80	13.33	0.79	0.014	0.337	0.615	0.300
8.833	0.0206	82.6	0.80	13.35	0.79	0.015	0.337	0.608	0.300
8.944	0.0203	82.7	0.80	13.36	0.79	0.015	0.337	0.602	0.300
9.056	0.0201	82.8	0.80	13.38	0.79	0.015	0.337	0.595	0.300
9.167	0.0198	82.9	0.80	13.40	0.79	0.015	0.337	0.589	0.300
9.278	0.0196	83.0	0.80	13.41	0.79	0.015	0.337	0.584	0.300
9.389	0.0194	83.1	0.80	13.43	0.79	0.015	0.337	0.578	0.300
9.500	0.0191	83.2	0.80	13.44	0.79	0.015	0.337	0.573	0.300
9.571	0.0190	83.2	0.80	13.45	0.79	0.015	0.337	0.568	0.300
9.643	0.0189	83.3	0.80	13.46	0.80	0.015	0.337	0.565	0.300
9.714	0.0187	83.3	0.80	13.47	0.80	0.015	0.337	0.562	0.300
9.786	0.0186	83.4	0.80	13.48	0.80	0.016	0.337	0.559	0.300
9.857	0.0184	83.4	0.80	13.49	0.80	0.016	0.337	0.556	0.300
9.929	0.0183	83.5	0.80	13.49	0.80	0.016	0.337	0.553	0.300
10.000	0.0182	83.5	0.80	13.50	0.80	0.016	0.338	0.550	0.300

```
*STOP*
($MAIN$)200+2
```

Distribution

Brobeck and Associates - Berkeley

Brobeck, W. M.

E. I. DuPont de Nemours and Company

Miner, L.
Sturgeon, D. L. G.

Electric Power Research Institute

Pepper, J. W.

Energy Research and Development Administration - Oak Ridge

Hickman, H. D.
Kiser, E. B.
Leed, R. E.
Zachry, D. S., Jr

Energy Research and Development Administration - Washington

Barber, K. F.
Chang, G. C.
Pezdirtz, G. F.

Garrett Corporation - Los Angeles

Raynard, A. E.

General Electric Research Center

Lustnader, E. L.

Johns Hopkins University-Applied Physics Laboratory

Rabenhorst, D. W.

Lawrence Livermore Laboratory

Chiao, T. T.
Christensen, R. M.
Schwartz, M. W.
Stone, R. G. (2)
Toland, R.
Wu, E. M.

Marshall Oil Company - Wake Forest

Marshall, H. K. (2)

National Aeronautics and Space Administration-Lewis

Schwartz, H. J.

National Aeronautics and Space Administration-Langley Research Center

Anderson, W. W.
Groom, N. J.

Naval Air Propulsion Test Center

Mangano, G. J.

Oak Ridge Gaseous Diffusion Plant

Babelay, E. F., Sr
Cuddy, L. M.
Keyser, R. M.
Morton, T. L.
Stief, S. S.
Waters, D. A.
Wilcox, W. J., Jr

Oak Ridge National Laboratory

Anderson, T.
Beall, S. E.
Callahan, J. P.
Dodge, W. G.
Fanning, D. N.

Oak Ridge Y-12 Plant

Alvey, H. E.
Babelay, E. F., Jr
Bernander, N. K.
Burditt, R. B.
Duggan, H. G.
Foulk, D. L.
Fraser, R. J.
Gray, J. R.
Gritzner, V. B.
Hensley, C. E.
Huddleston, R. L. (10)
Jones, F. W.
Kahl, K. G.
Keith, A.
Kelly, J. J. (10)
Kite, H. T. (25)
Knight, C. E., Jr (10)
Martin, W. R./Googin, J. M.
Mason, D. L./Schreyer, J. M.
Mills, J. M., Jr
Oliphant, G. W.
Perry, A. E.
Phillips, L. R.
Post, D. W.

Rhew, J. E.
Smith, H. F., Jr
Smith, R. D.
Stoner, H. H./Butturini, W. G./Dritt, W. S.
Tewes, W. E.
Thompson, W. F.
Tilson, F. V.
Tunnell, H. H.
White, B. J.
Whitson, W. K.
Yaggi, W. J.
Y-12 Central Files (master copy)
Y-12 Central Files (route copy)
Y-12 Central Files (Y-12RC)
Y-12 Central Files (5)

Owens Corning Fiberglas

Loud, S. N.

Paducah Gaseous Diffusion Plant

Bewley, H. D.

Public Service Electric and Gas Company

Schneider, T. R.

Rockwell International - Canoga Park

Davis, D. E.

Rockwell International - Downey

Notti, J. E.

Sandia - Albuquerque

Braasch, R. H. (2)
Gerstle, F. P.
Reuter, R. C.

Sandia - Livermore

Hargreave, R. M.

Tennessee Valley Authority

Siegel, G. R. (2)

University of Wisconsin - Madison

Frank, A. A.

US Army - Fort Belvoir

Amstutz, L. I. (USAMERADCOM)

US Flywheel, Inc - San Juan, California

Swartout, B. E.

In addition, this report is distributed in accordance with the Category UC-94b, **Energy Storage—Mechanical**, as given in the *USERDA Standard Distribution Lists for Unclassified Scientific and Technical Reports*, TID-4500.

☆ U.S. GOVERNMENT PRINTING OFFICE: 1977-748-189/210